THE ASTROPHYSICAL JOURNAL, 494:724–733, 1998 February 20

A SEARCH FOR HARD-SPECTRUM GAMMA-RAY BURSTS USING *SMM*

MICHAEL J. HARRIS
Universities Space Research Association, 300 D Street S.W., Suite 801, Washington, DC 20024
AND
GERALD H. SHARE
Code 7652, Naval Research Laboratory, Washington, DC 20375-5320
Received 1997 May 5; accepted 1997 October 1

ABSTRACT

We have searched over 9 yr of data from the *Solar Maximum Mission* (*SMM*) Gamma Ray Spectrometer for gamma-ray bursts (GRBs) with abnormally hard spectra that may have been missed in previous searches in the 0.35–0.8 MeV energy band. For this purpose, we searched the higher 0.8–10 MeV band. We have found only two new GRBs in this search, compared to 177 GRBs found in the 0.35–0.8 MeV band. We have made a careful examination of the threshold conditions for identifying the 0.8–10 MeV events, which confirms that there is no undiscovered population of hard-spectrum GRBs that have escaped detection by *SMM*, BATSE, and other instruments triggered by low-energy γ-ray emission. This conclusion does not apply to GRBs with duration less than 2 s, nor to those that are much fainter than the general population. Our results constrain models of GRBs that require or allow the peak in energy emission to be above 1 MeV.

Subject headings: gamma rays: bursts — surveys

1. INTRODUCTION

The origin of gamma-ray bursts (GRBs) remains one of the outstanding problems in astrophysics today (Fishman & Meegan 1995). The discovery of GRBs emitting photons with energies above 1 GeV (e.g., Hurley et al. 1994; Dingus 1995) has spurred further interest in high-energy emissions (>1 MeV) from bursts. "Traditional" GRBs are typically identified by sharp increases in the count rates in the 50–200 keV band. Although some of these bursts have been observed up to energies near 100 MeV (e.g., Share et al. 1986), concerns have been voiced that a whole class of bursts may have been missed due to use of the hard X-ray band for identifying GRBs (e.g., Piran & Narayan 1996). If the current detection strategy discriminates against bursts with harder than average spectra, then there may exist GRBs that emit strongly at energies ≥ 1 MeV, but whose emission near 100 keV falls below detection thresholds.

The spectral hardness H of a GRB spectrum is defined as the position of the peak in νf_ν (power emitted per decade in energy). Traditional GRBs have notoriously featureless spectra, which make such peaks broad and hard to define, as they are merely slight "breaks" in otherwise power-law spectra. However, Band et al. (1993) have analyzed the spectra of 54 GRBs observed by the Burst and Transient Source Experiment (BATSE) on the *Compton Gamma Ray Observatory* and have shown that the spectra tend to exhibit broad peaks in νf_ν at energies of a few hundred keV. Their results are illustrated in Figure 1*a*, which is a three-dimensional plot of the number of GRBs versus H and mean 0.03–2 MeV flux, F; the same data are also shown as contours in Figure 1*b*. The distribution has a broad peak around $H \simeq 200$ keV and $F \sim 5$ photons cm^{-2} s^{-1}. From this peak the GRB frequency falls off in four directions. The distribution toward low fluxes is incomplete due to BATSE's loss of sensitivity for faint GRBs. The falloff toward high fluxes is probably real—all measured luminosity functions show a relative lack of bright GRBs in nature. The falloff toward low hardnesses is also real; it reflects the well-known deficiency in traditional GRB spectra at X-ray energies.

The cause of the falloff of the frequency distribution toward higher hardnesses is the problem addressed in this paper. In the hypothesis of Piran & Narayan (1996), this falloff is due entirely to a loss of detection efficiency in instruments that detect GRBs using low-energy triggers. Piran & Narayan (1996) analyzed the expected response of BATSE to GRB distributions following power-law models in log H and in logarithm of bolometric luminosity, and found that the data suggest that one or both of the power-law indices must be positive or at least zero. In other words, the number of bursts per decade of hardness either increases with increasing H, or else is constant with H if harder GRBs are more luminous. The dashed line in Figure 1*a* represents a hypothetical distribution of GRBs that is constant with hardness H; it is normalized at the peak of the contour distribution observed by BATSE. Comparison of this hypothetical distribution with the BATSE observations suggests that there must be a large class of undiscovered "MeV bursts" if the Piran & Narayan (1996) hypothesis is correct. This new class may contain events quite distinct from the traditional population. For example, such GRBs would be candidates for the group of long-lasting bursts emitting above 1 MeV that Katz & Canel (1996) have proposed as signatures of a new class of accretion-induced white dwarf collapse events.

In this paper we use data from the *Solar Maximum Mission* Gamma Ray Spectrometer (*SMM* GRS) to demonstrate that such a hard class of GRBs does not exist. This is possible because the experiment has good sensitivity to GRBs above 1 MeV and permits searches for new bursts at both higher and lower energies. We can therefore avoid many complications involved in comparisons between different instruments by making comparisons solely between GRS measurements in different energy bands. Whether or

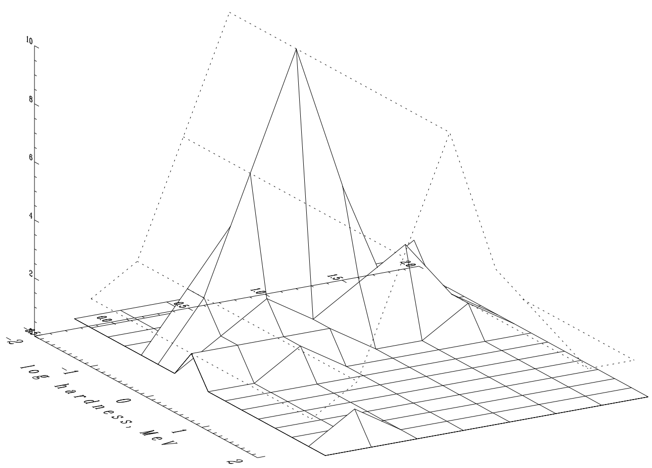

FIG. 1*a*

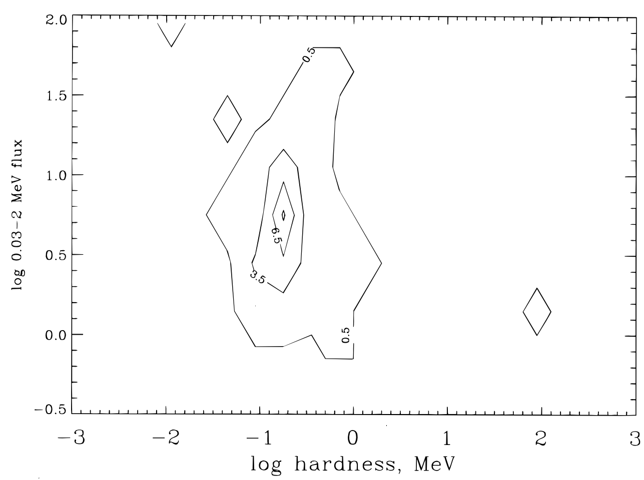

FIG. 1*b*

FIG. 1.—(*a*) Three-dimensional distribution of 54 GRBs detected by BATSE and analyzed by Band et al. (1993) from low-energy (50–200 keV) triggers, binned by logarithm of spectral hardness and logarithm of 0.03–2 MeV flux in 0.3 decade bins. *Dashed lines:* Expected distribution of GRBs as a function of spectral hardness and 0.03–2 MeV flux, according to the prediction of Piran & Narayan (1996) that it is a constant with hardness for all GRB fluxes, normalized to the peak in the observed distribution at a given flux. (*b*) Same data as (*a*) expressed as a contour plot.

not the hypothesis of Piran & Narayan (1996) is valid, a study of this kind is important to the understanding of the GRB enigma.

2. BURST DETECTION IN *SMM* DATA

2.1. *Mission and Instrument Characteristics*

The *SMM* GRS was in low Earth orbit during the period from 1980 March to 1989 December. Although it was pointed at the Sun for almost the whole of this time, its field of view (FOV) was so large ($\simeq 150°$ at 1 MeV), and its shielding so relatively modest, that it was an effective burst monitor for the whole sky. Data were accumulated continuously, except during passages of the South Atlantic Anomaly (SAA), during brief calibration periods, and during most of the 5 month period from 1983 November to 1984 April when the satellite's tape recorder was turned off prior to its repair. Seven 7.5×7.5 cm NaI detectors returned data in 476 energy channels between 0.3 and 10 MeV; a 5 cm thick CsI shield lying just below these detectors could be used in combination to obtain spectral measurements from 10 to 100 MeV in four broad energy bands.

With these characteristics, the instrument performed capably as a GRB detector, and some important measurements were made with it. For example Matz et al. (1992) and Higdon et al. (1992) were able to measure the bursts' V/V_{max} distribution, determining that GRBs are not homogeneously distributed; Nolan et al. (1984) and Messina & Share (1992) did not confirm previously reported γ-ray line emission, casting doubt on the theory that the bursts occur on the surfaces of Galactic neutron stars. Of greater relevance to the present study, Share et al. (1982) and Matz et al. (1985) showed that a large fraction of GRBs emit at energies greater than 1 MeV, and later detected emission greater than 10 MeV for the first time (Share et al. 1986). These discoveries exploited the GRS's combination of extensive sky coverage and sensitivity to photon energies above 1 MeV.

The drawbacks of the GRS as a burst detector were its very poor spatial and temporal resolutions. The poor spatial resolution was a consequence of the wide FOV described above; it was virtually impossible for the GRS to locate any GRB, except to the extent that Earth blocked a known portion of the FOV. The spectral data were returned in a continuous stream in 16.384 s intervals, i.e., longer than the durations of most GRBs (1–10 s). Our analysis (§ 2.4) takes into account the GRS's poor spatial resolution but cannot fully correct for its limited time resolution. There is therefore a possibility that our search for high-energy bursts will be incomplete for GRBs with durations much shorter than 16 s.

2.2. *Bursts Discovered at Energies* 0.35–0.8 MeV

A published catalog of GRBs observed by the *SMM* GRS has yet to be completed; however, the methods used for detecting GRBs, and some of their characteristics, were described by Share et al. (1992). Most of the GRBs were detected by an automated search covering the 350–800 keV energy range at 16 s resolution; the search was performed over limited ranges in geomagnetic rigidity in order to reduce false triggers due to background changes on orbital ($\simeq 90$ minutes) timescales. A quadratic function was fitted to the rates, and candidate transient events were flagged when excesses greater than 5.7 σ occurred in 16 s intervals, or else when acceptable fits could not be made. A total of ~ 8000 transients were detected. These transients were then visually inspected to identify true GRBs. About 3000 of these transients were from γ radiation emitted by Soviet nuclear-powered reconnaissance satellites (Rieger et al. 1989; Share et al. 1989); 80% of these occurred in 1987 and 1988. Solar flares were identified by reports in Solar Geophysical Data and by their intense thermal emission recorded in the 13–19 keV band of GRS's small X-ray detectors. The remaining transients were primarily due to data and telemetry errors and to precipitating electrons during geomagnetically disturbed periods; these were easily distinguishable from GRBs.

A total of 177 GRBs were detected in the 0.35–0.8 MeV band. Of these, 136 were identified by the computer algorithm. The remaining bursts were identified during visual screening of the entire database and from GRBs reported by other spacecraft. Time-integrated spectra of the bursts were obtained by subtracting backgrounds adjacent to and on both sides of the burst. Preliminary fits to these spectra used representative shapes such as a power-law, thermal bremsstrahlung, and thermal synchrotron (Share et al. 1992). These photon models were convolved with the instrument response function before fitting to the data using a χ^2-minimization algorithm. As the locations of the sources of the GRBs were not known, fits were performed for assumed incidence angles of both 0° and 90°. It is important for our analysis in this paper to note that *fits at 0° incident angle yield the hardest incoming GRB spectra.* This is because at other angles low-energy photons are more strongly attenuated, so the unfolded spectra become steeper (in other words, for a given observed spectrum, more soft photons are assumed to be added to obtain the real spectrum). Thus by assuming an incident angle of 0° we provide upper limits to the spectral hardness of the GRBs, which we will refer to as H_0.

The hardest GRS burst spectrum had a power-law index ~ -1.3 and the softest an index ~ -3.8 for 0° incidence angle. Improved fits to many spectra were achieved by using shapes, such as the thermal synchrotron (TS) function, which describe spectra having convex curvature at energies between a few hundred keV and a few MeV. One burst, GRB 840805, required an additional power-law component at high energy. This latter model is similar to the general form used for fitting the bursts observed by BATSE (Band et al. 1993).

The BATSE data suggest that GRB spectra tend to exhibit broad peaks in νf_ν at energies of a few hundred keV. We therefore used the results derived from fits with the thermal synchrotron model in this study. It is not suggested that synchrotron emission is the preferable physical explanation for the spectra; the TS shape gives relatively good fits to the data, and the results were available to us from previous work. The spectral fits are in fact rather insensitive to the precise shape of the model, so long as it exhibits the required broad peak in νf_ν. The hardness H_0 can therefore be defined for any fitted spectrum.

2.3. *Search for Very Hard GRBs*

The same computer algorithm was employed to search for bursts in the 0.8–2 MeV and 2–10 MeV bands as was described above for the 0.35–0.8 MeV band search. This procedure yielded a very large number of false positive detections. There were ~ 7000 transient events identified in one or both energy ranges. These were individually screened using microfilm records of the database providing both rates in broad energy bands and 5 minute accumulated spectra. Most of the transients were found to be due to errors in data transmission, manifesting themselves as sharp increases in single GRS energy channels. About 50 events were caused by lack of adequate background determinations used by the algorithm due to data gaps arising from telemetry losses, SAA passages, and instrument calibrations.

A sample of about 250 transient events remained after these primary screenings. Of these, more than half (160) were due to γ-ray emission from Soviet nuclear reactors when they approached to within 800 km of *SMM* (Share et al. 1989). Thirty of the remainder were GRBs originally identified in the 0.35–0.8 MeV search described in the previous section. A further 50 events consisted of high-energy solar flares, magnetospheric disturbances, and other events dominated by charged particles (as measured by plastic scintillation detectors).

A total of only five unexplained events remained. Spectra for these events were extracted and corrected for background as discussed in § 2.2 above. Inspection of three of the background-corrected spectra revealed the presence of high counts in individual channels, (once again indicating data transmission errors) or of systematic negative fluxes at some energies (revealing the failure of the background-subtraction procedure). None of them showed significant positive emission from the whole of the range 0.8–10 MeV. These three events were therefore also discarded.

Thus, out of our intensive search for new 0.8–10 MeV transients in the 10 yr *SMM* database, we have only identified two new candidate high-energy gamma-ray bursts. Time histories of these two events, GRB 820329 and GRB 840906, are plotted in Figures 2*a* and 2*b* for three broad energy bands (0.35–0.8, 0.8–2.0, and 2.0–8.5 MeV). The burst durations were about 80 and 64 s, respectively. It is clear from these plots why these events were not detected by the computer search of the low-energy band, as the most significant emission occurs at higher energy and the events are extended in time. The time-integrated spectra for these events are plotted in Figures 3*a* and 3*b*; the solid lines are fits to data for photon spectra represented by power laws and incident at 0°. Both events had harder spectra than any other detected by *SMM* from low-energy triggers, but only marginally so. The power-law indices of the new bursts were -1.05 ± 0.04 and -1.03 ± 0.30 for GRB 820329 and GRB 840906, respectively. (The TS fits were not significantly better or worse than the power-law fits. They yielded spectral hardnesses $H_0 \geq 10$ MeV for 0° incidence angle for both bursts.) By comparison, the hardest GRB spectrum, GRB 821028, found in the 0.35–0.8 MeV search had an index -1.27 (Share et al. 1992); its spectrum is plotted in Figure 3*c*. Also shown for comparison in Figure 3*d* is the spectrum of GRB 840805 that was detected up to ~ 80 MeV.

Neither of the two new events was detected by any other spacecraft in operation at the time. In general the reason for this was the same very hard spectra that caused the GRS low-energy search to miss them. The detectors on board *PVO*, *International Cometary Explorer* (*ICE*), and the *Venera* missions triggered at even lower energies (≤ 150 keV) than the GRS, and even an intense burst would not deposit much energy in this range if its spectrum were very hard. For example, the spectrum of GRB 820329 in Figure 3*a*, if extrapolated downward to the *PVO* trigger energy band 0.1–0.2 MeV, contains less than the 2×10^{-5} ergs cm^{-2} s^{-1} typically necessary for a trigger (Fennimore et al. 1993).

2.4. *Threshold for Burst Detection above* 0.8 MeV

In order to assess properly the possible existence of a class of hard GRBs, we need to understand the GRS's sensitivity for discovering bursts at energies above 0.8 MeV. We obtained a sample of about 70 "null" spectra from events identified in our search for hard GRBs. We used this sample to compute the effective threshold for detecting GRBs under a broad range of conditions. The GRS's sensitivity depends upon parameters that may be either (1) intrinsic to the spacecraft and environment, e.g., geomagnetic rigidity, γ radiation from Earth's atmosphere, and induced radio-

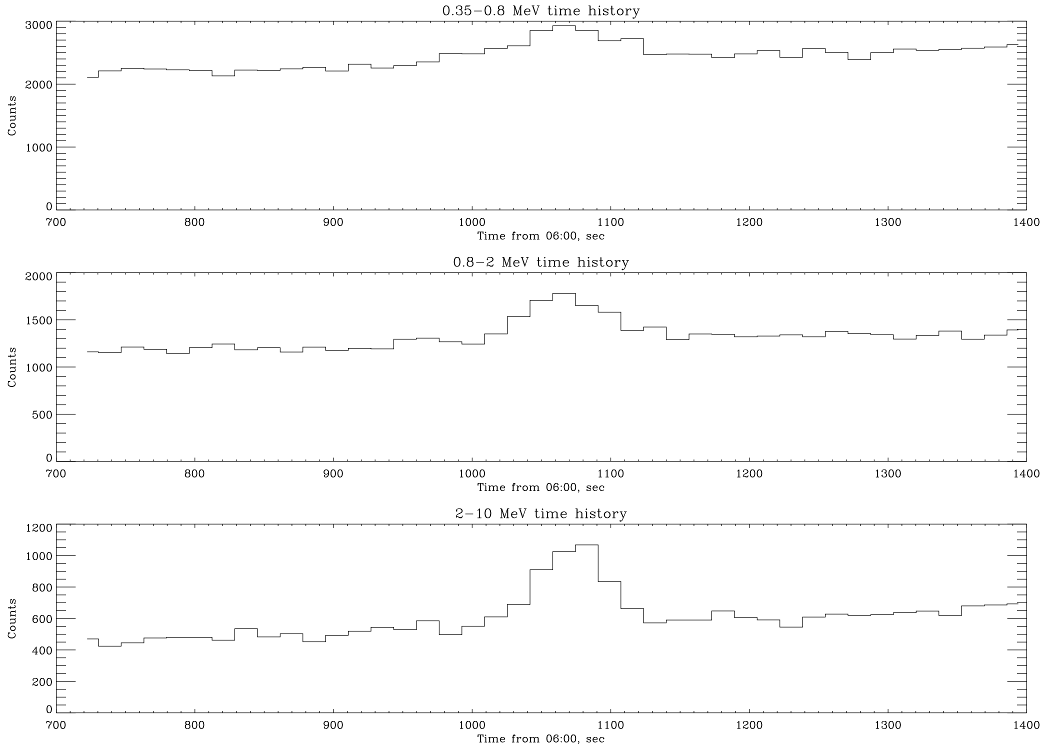

FIG. 2*a*

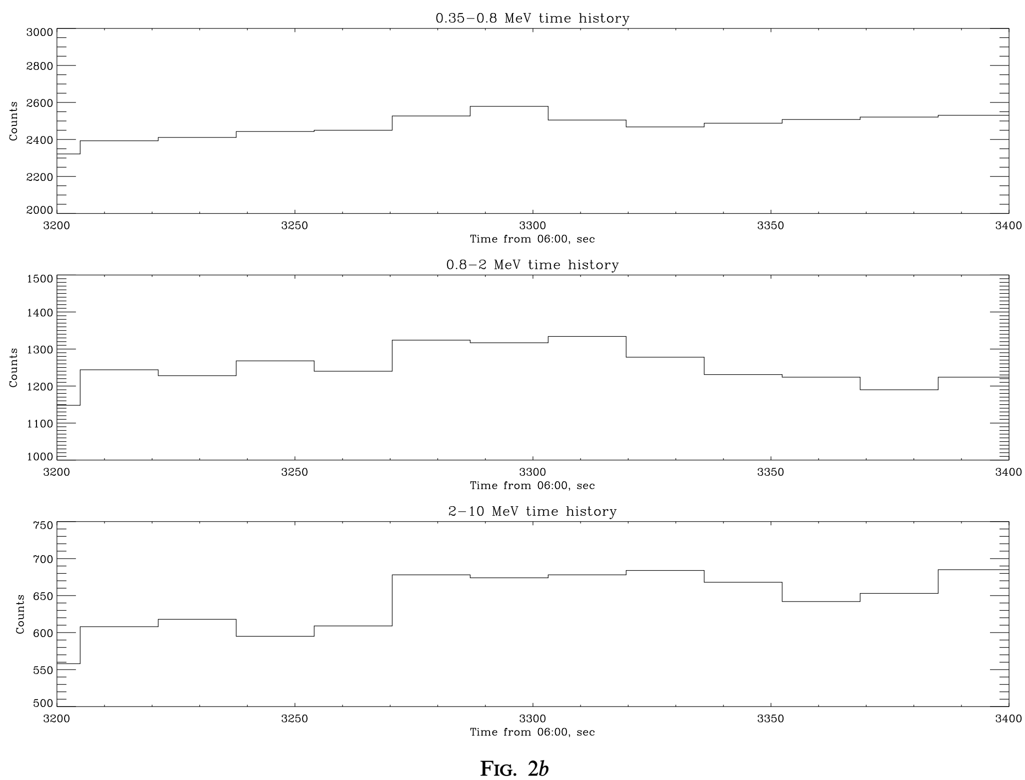

FIG. 2*b*

FIG. 2.—(*a*) Count rates in three energy bands (*top*, 0.35–0.8 MeV; *middle*, 0.8–2 MeV; *bottom*, 2–10 MeV) for new hard-spectrum GRB 820329, in 16.384 s intervals. (*b*) Count rates in the same three energy bands as (*a*) for new GRB 840906.

activity from SAA passages and long-term cosmic-ray irradiation, or (2) intrinsic to the burst itself—the GRB duration, the spectral hardness, and the location of the GRB within the FOV.

Studies of the variation of spacecraft and environmental backgrounds in the GRS, on different timescales (e.g., Dunphy et al. 1989; Kurfess et al. 1989) indicate that it causes the GRS's sensitivity to bursts to vary by no more

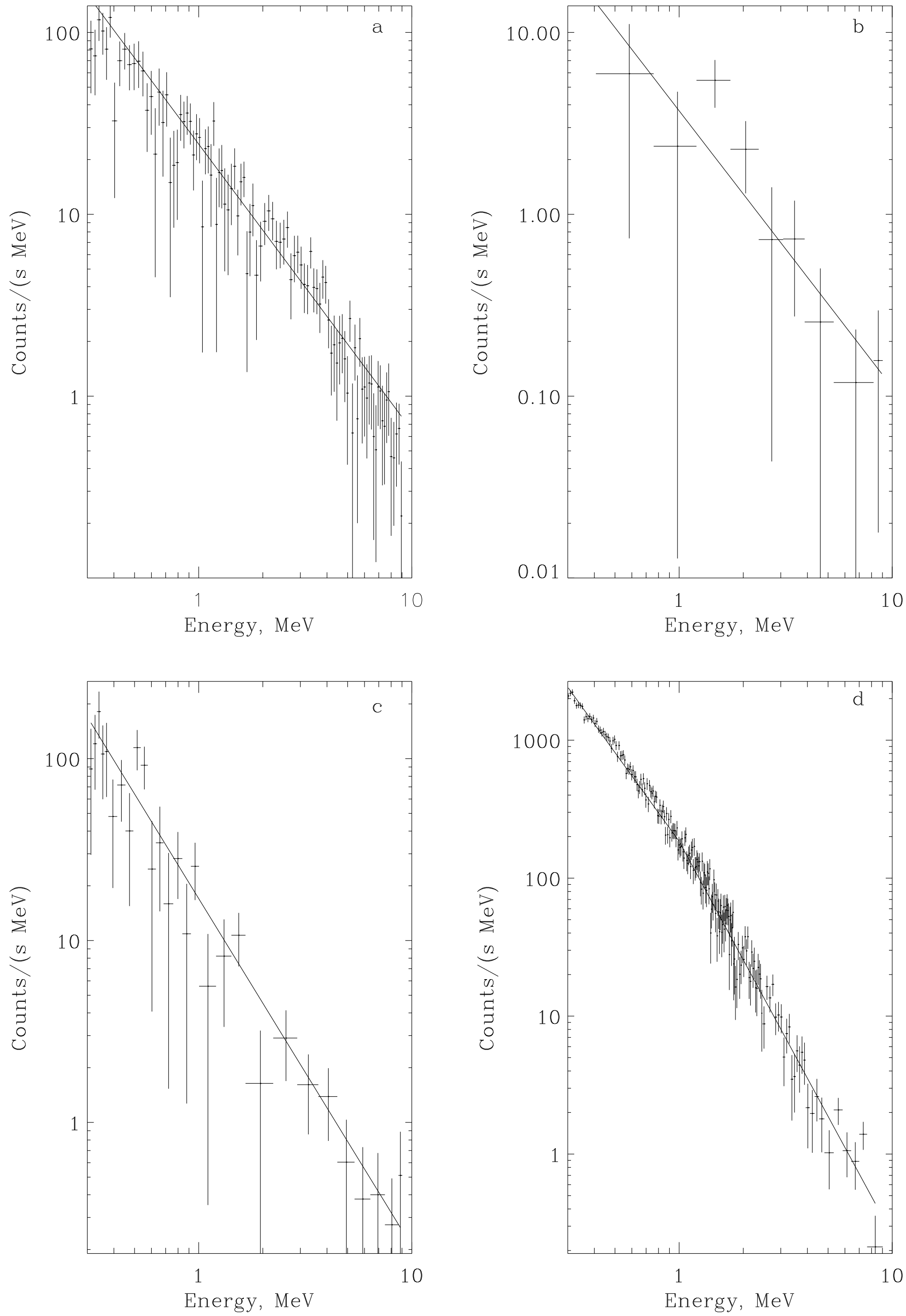

FIG. 3.—(*a*) *SMM* GRS spectrum of new hard-spectrum GRB 820329 between 0.3 and 8.5 MeV. *Continuous line:* Power-law spectrum $(6.4 \pm 0.2) \times 10^{-2}$ $(E/1.6\ \mathrm{MeV})^{-1.05 \pm 0.04}$ photons $\mathrm{cm^{-2}\ s^{-1}\ MeV^{-1}}$ fitted assuming 0° incidence angle. (*b*) *SMM* GRS spectrum of new GRB 840906 between 0.3 and 8.5 MeV. *Continuous line:* Power-law spectrum $(1.1 \pm 0.3) \times 10^{-2}$ $(E/1.6\ \mathrm{MeV})^{-1.03 \pm 0.30}$ photons $\mathrm{cm^{-2}\ s^{-1}\ MeV^{-1}}$ assuming 0° incidence angle. (*c*) *SMM* GRS spectrum of GRB 821028, the hardest spectrum measured by Share et al. (1992), between 0.3 and 8.5 MeV. *Continuous line:* Power-law spectrum $(6.8 \pm 0.6) \times 10^{-2}$ $(E/1.6\mathrm{MeV})^{-1.27 \pm 0.09}$ photons $\mathrm{cm^{-2}\ s^{-1}\ MeV^{-1}}$ assuming 0° incidence angle. (*d*) *SMM* GRS spectrum of GRB 840805, the spectrum extending to the highest energy (80 MeV: Share et al. 1986, 1992), between 0.3 and 8.5 MeV. *Continuous line:* Broken power-law spectrum assuming 0° incidence angle with amplitude 1.08 ± 0.02 photons $\mathrm{cm^{-2}\ s^{-1}\ MeV^{-1}}$ at 1 MeV, with indices -1.94 ± 0.06 below 1 MeV and -2.25 ± 0.06 above 1 MeV.

than a factor ~ 2. This was confirmed by fitting power-law spectra to the sample of 70 null spectra and examining the dependence of the results on the *SMM* environment parameters. From these events we estimate a mean 3 σ threshold sensitivity of about 4×10^{-2} photons $\mathrm{cm^{-2}\ s^{-1}}$ between 0.8 and 10 MeV, for bursts of 16 s duration and 0° incidence angle.

We next consider the effect on sensitivity of the quantities intrinsic to the GRBs. Bursts have durations t lasting from tenths to tens of seconds. We expect that the sensitivity will vary as $t^{-1/2}$, and this is confirmed by our spectral fits to null events selected to be of varying lengths between 16 and 96 s. As the GRS's temporal resolution is 16 s, we need to correct its sensitivity by the mean value of $(t/16\ \mathrm{s})^{-1/2}$ aver-

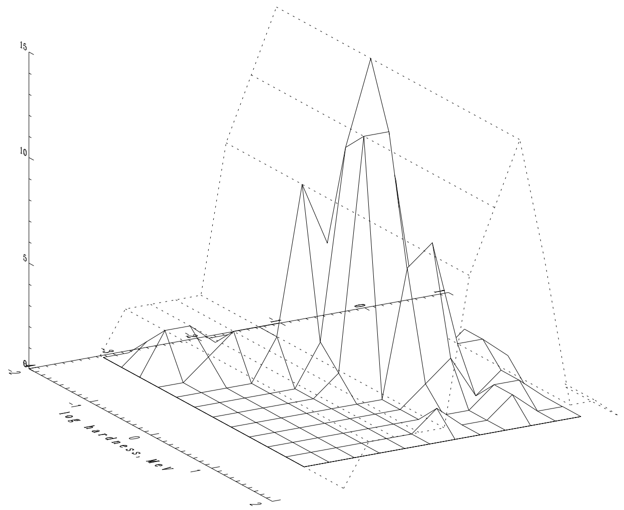

FIG. 4*a*

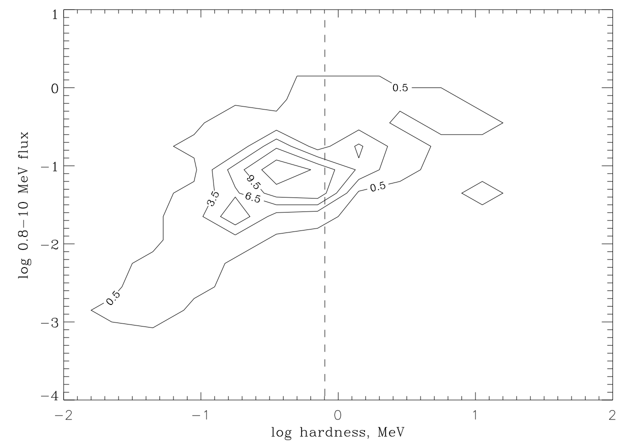

FIG. 4*b*

FIG. 4.—(*a*) Distribution of 138 GRBs detected by *SMM* during 1980–1989, as a function of spectral hardness and 0.8–10 MeV flux in the form of a three-dimensional surface. *Dashed line:* Expected distribution of GRBs visible to *SMM* according to Piran & Narayan (1996) (constant with hardness and normalized to peak in the observed distribution at a given flux). (*b*) Same data as (*a*) expressed as a contour plot. *Dashed line:* Hardness value $H_0 = 0.8$ MeV above which GRB distribution will be compared to Piran & Narayan prediction (i.e., dashed line in [*a*]).

aged over the distribution of durations of GRBs. Data from the large area detectors of BATSE (Kouveliotou et al. 1993) confirmed that this distribution is bimodal, as previously suspected (Hurley 1992). There is a fairly well-defined boundary between the resulting two subclasses of GRBs at a duration of 2 s. This is close to the minimum measurable duration of the GRBs detected by *SMM*, which is 4 s.[1] Since the GRS's sensitivity is proportional to $t^{-1/2}$ for durations less than 16 s, it is clear that the GRS will have very little sensitivity to the shorter of the two subclasses. Our conclusions will therefore apply only to the longer subclass (≥ 2 s) found by Kouveliotou et al. (1993).

There is a further reason for excluding the class of very short GRBs from this study. Even if the GRS's sensitivity extended down to short GRB durations, our analysis would not be valid if there were an anticorrelation between hardness and duration—very hard, very short GRBs would be missed by BATSE due to their hardness and by *SMM* due to their shortness. An anticorrelation of this kind was found by Kouveliotou et al. (1993) in the subclass of short (< 2 s) GRBs. On the other hand, Dezalay et al. (1996) found a *positive* correlation between durations and hardness for the subclass of longer (≥ 2 s) events in the BATSE and PHEBUS data. The BATSE spectroscopy detector sample that was analyzed in the Piran & Narayan (1996) study also showed a positive correlation (Band et al. 1993); it sampled roughly the same range in burst durations as the *SMM*/GRS, corresponding to the longer subclass.

Components of GRB emission that emerge on very long timescales are also undetectable by our analysis, which is restricted to times less than a few hundred seconds by changing backgrounds on orbital timescales. The detection of very hard emission by EGRET from GRB 940217 over an interval of 5400 s (Hurley et al. 1994) implies the existence of such a component. It is not clear, however, that it is ever seen on its own; in GRB 940217 it was accompanied by variability at lower energies on short timescales that our analysis would detect. This is another possible limitation on the completeness of our results.

The second intrinsic factor to be considered is spectral hardness. We estimated the dependence of threshold sensitivity on spectral hardness by repeating our fits to 70 null spectra using six different TS model spectra with hardness values between 0.8 and 10 MeV. Once again we assumed a 0° incidence angle for the source. As argued in § 2.2, *this assumption is the most conservative*, *since it yields the largest value for the hardness of the GRB*. We treated this dependence on hardness explicitly, and will present separate results for each of the six hardness values in the next section.

The largest single factor affecting the threshold sensitivity is the third of the intrinsic GRB properties: the lack of knowledge of the location of GRBs within the GRS FOV. We calculated the efficiency of the GRS as a function of incident angle, relative to that at 0° for the six TS model spectra having hardnesses between 0.8 and 10 MeV, using Monte Carlo simulations of the energy and angle dependence of the GRS response (S. M. Matz & G. V. Jung 1986, private communication). The threshold sensitivity was found to vary by factors of 5–7, depending on the spectral hardness, and is always degraded at other angles relative to 0° incidence.

3. RESULTS

The primary objective of this paper is to determine whether there is a class of GRBs with hard spectra that have been missed in previous searches. We showed that such a class is not evident in the distribution of bursts observed by the BATSE spectroscopy detectors and plotted in Figure 1. We perform a similar analysis in this section using the higher *SMM*/GRS energy bands, and demonstrate that such a class is not evident in these data either. Since the triggering criteria, spectral ranges, and timescales are different, we will not attempt to merge the results of the *SMM*/GRS and BATSE instruments.

Plotted in Figure 4 is the distribution of the 136 GRBs found by computer in the original search in the 0.35–0.8

[1] These measurements were accomplished independently of the GRS, using two 10–140 keV X-ray monitors attached to the GRS for the purpose of monitoring solar flares.

MeV band (§ 2.2), plus the two GRBs found by our comparable search at energies greater than 0.8 MeV (§ 2.3). The distribution is plotted in a three-dimensional format in Figure 4*a* and as a contour in Figure 4*b*, similar to Figure 1. The numbers of bursts are plotted in bins of 0.3 decades as a function of spectral hardness H_0 (hardness derived for 0° incidence) and of mean flux in the 0.8–10 MeV energy band (we assume this is equivalent to the bolometric flux, which is justified for the GRBs with $H_0 \geq 0.8$). The most noticeable feature is a marked decrease in burst frequency with increasing hardness above a broad peak at $H_0 \simeq 0.5$ MeV; the peaking resembles that found by BATSE (Band et al. 1993; see Fig. 1), with the exception that the GRS data span a broader range of spectral hardness.

According to the model of Piran & Naryan (1996), one would expect the rate of bursts at any bolometric luminosity to remain at least constant for hardnesses above the peak in the distribution. Plotted by the dashed lines in Figure 4*a* is a representation of this expectation, normalized to the peak of the distribution at every luminosity. It is clearly at variance with the distribution of *SMM* bursts, as it was for the BATSE bursts. Note that the hardnesses H_0 plotted in Figure 4*a* are in fact upper limits because of our assumption of 0° incidence angle (§ 2.2). In reality the entire distribution should be shifted to lower H if a range of incident angles is assumed, thus exacerbating the disagreement with the Piran & Naryan (1996) model.

3.1. *Is the Deficiency of GRBs with Spectral Hardness Intrinsic?*

It is important to determine whether the observed falloff in the numbers of GRBs at energies above 0.8 MeV is due to a lack of sensitivity of the search or is intrinsic to GRBs. For this reason we use our sensitivity studies discussed in § 2.4 to answer this important question.

We found in § 2.4 that the distribution of GRS threshold sensitivities for each hardness is due mainly to its angular response, with a relatively small variation due to the local background. In Figure 5 we show the GRS's probability for detecting at the 3 σ level GRBs randomly located in the aperture for each of six values of hardness (the same for which we made detailed sensitivity calculations in § 2.4, between 0.8 and 10 MeV). These probabilities were obtained by calculating the efficiency of the GRS as a function of energy and of incidence angle, relative to that at 0°, from S. M. Matz & G. V. Jung's (1986, private communication) Monte Carlo calculations. For discrete values of incidence angle at 10° intervals, we calculated the overall efficiency of the GRS for each hardness, integrating over the efficiency as a function of energy (weighted by each energy's contribution to the TS spectrum of given hardness). We then calculated the distribution of efficiencies according to the area of the sky within a band $\pm 5°$ of each incidence angle.

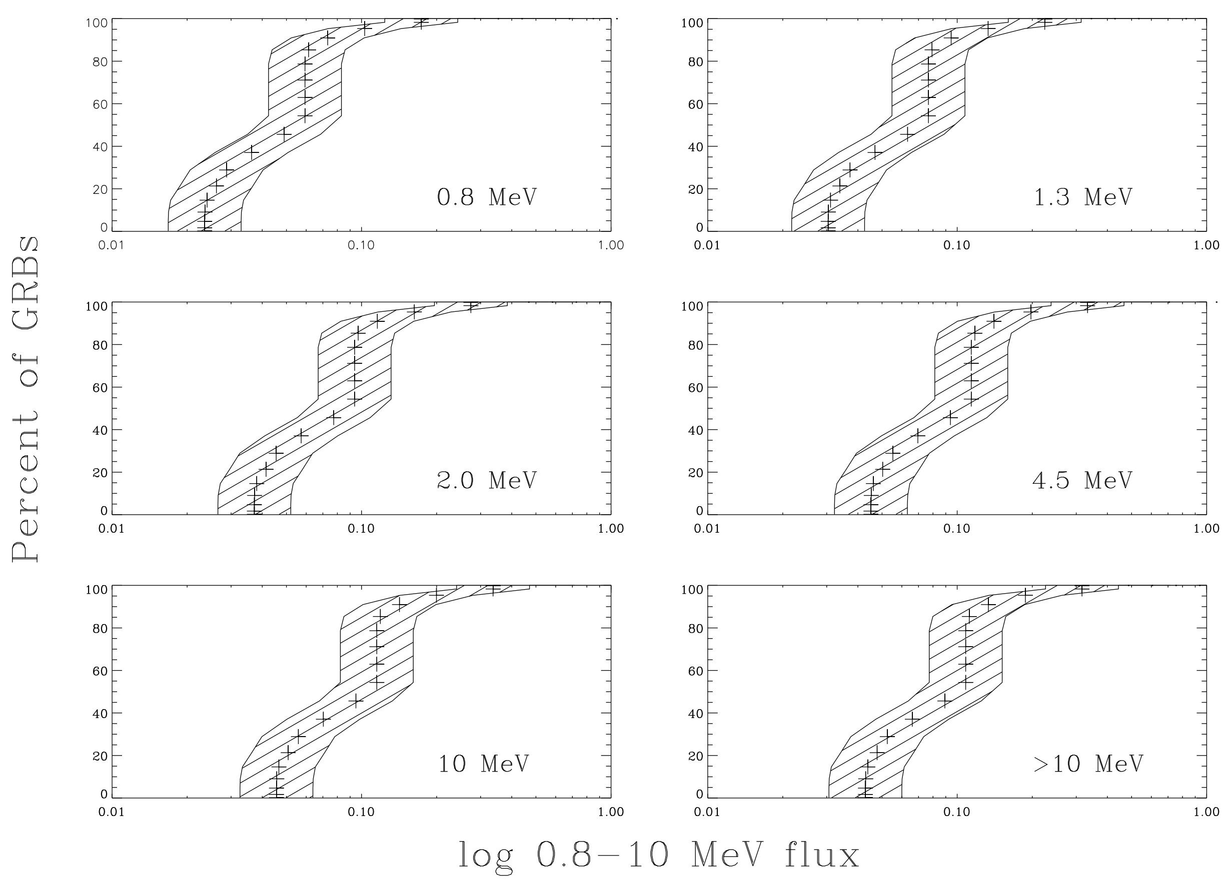

FIG. 5.—Percentage of GRBs detectable at significance $\geq 3\ \sigma$ by our current search as a function of burst average flux (*points*), for six values of spectral hardness. The effect of characteristic background variability is shown by the shading. Apart from this variability, the detection efficiency is assumed to depend only on the fraction of GRBs occurring (at random) at different off-axis distances in the GRS aperture. Shaded area represents variability in detection efficiency due to characteristic changes in spacecraft and detector backgrounds during the mission.

One can understand the plots in Figure 5 by realizing that the GRS has approximately its optimum response (the 0° value) out to a half-angle of $\sim 35°$; over this range we found that the average 3 σ sensitivity in flux in the 0.8–10 MeV range was $\sim 4 \times 10^{-2}$ photons cm^{-2} s^{-1} (§ 2.4). This value varies slightly with hardness, mainly due to our neglect of the bolometric correction to the 0.8–10 MeV band; as an example, for $H_0 \simeq 0.8$ MeV the 3 σ threshold is 2.4×10^{-2} photons cm^{-2} s^{-1}. All bursts with this hardness and with fluxes above this value should have been detected (leaving aside the variation of sensitivity by a factor of 2 due to local backgrounds—indicated by the width of the shaded region in Fig. 5). However, only $\sim 9\%$ of bursts distributed randomly on the sky will be detected with this high sensitivity. The angular response of the detector falls off by a factor of 2 by 90°, increasing the threshold to 5×10^{-2} photons cm^{-2} s^{-1}; however, fully 50% of the sky is contained within 90°, so that 50% of all GRBs should be detected to this sensitivity or better. The worst situation is toward the rear of the GRS at angles near 180°. The sensitivity is reduced here by a factor 7 (§ 2.4). All GRBs (100%) should be detected with this sensitivity or better.

We next use these sensitivity curves to correct the observed rates of hard GRBs from *SMM* (Fig. 4) to yield the total numbers of GRBs incident on the detector as a function of hardness and 0.8–10 MeV flux. This is performed by dividing the number of GRBs in each bin of Figure 4*a* by the averaged value of the detection probability in that bin from Figure 5. There are a total of 39 GRBs with $H_0 \geq 0.8$ MeV identified by *SMM* (37 found using the search of 0.35–0.8 MeV triggers, and two found in the present search). In Figure 6 (*histogram*) we plot the number of these GRBs as a function of flux for the six standard values of hardness after the correction for reduced sensitivity has been made.

These numbers can be directly compared to the expected rates according to Piran & Narayan (1996). The dashed line in Fig. 6 is the expected GRB rate during the *SMM* mission according to Piran & Narayan (1996), which by hypothesis is the same for all H_0 values (Fig. 4*a*). The Piran & Narayan predicted rate must be at least as large as the GRB rate seen at *any* hardness. It is conservative to minimize this predicted rate; it is therefore normalized to the peak *SMM* event rates in Figure 4*a*, which occur at lower hardnesses $\simeq 0.5$ MeV (the correction factor being assumed to be unity at these hardnesses). For example, in the 0.8–10 MeV flux bin around 0.1 photons cm^{-2} s^{-1} the peak GRB rate is 15 events around $H_0 = 0.5$ (Fig. 4*b* and dashed curve in Fig. 6); around hardness $H_0 = 0.8$ a rate of 12 events was measured in this bin (Fig. 4*b*); the detection probability for this hardness and flux is 93% (Fig. 5, $H_0 = 0.8$); therefore, correcting the measured rate of bursts for this factor yields a true rate of 12.9 events, to be compared to the expected rate of 15 (Fig. 6, $H_0 = 0.8$).

It is clear from Figure 6 that, for all except the lowest hardness values, the incident number of bursts determined

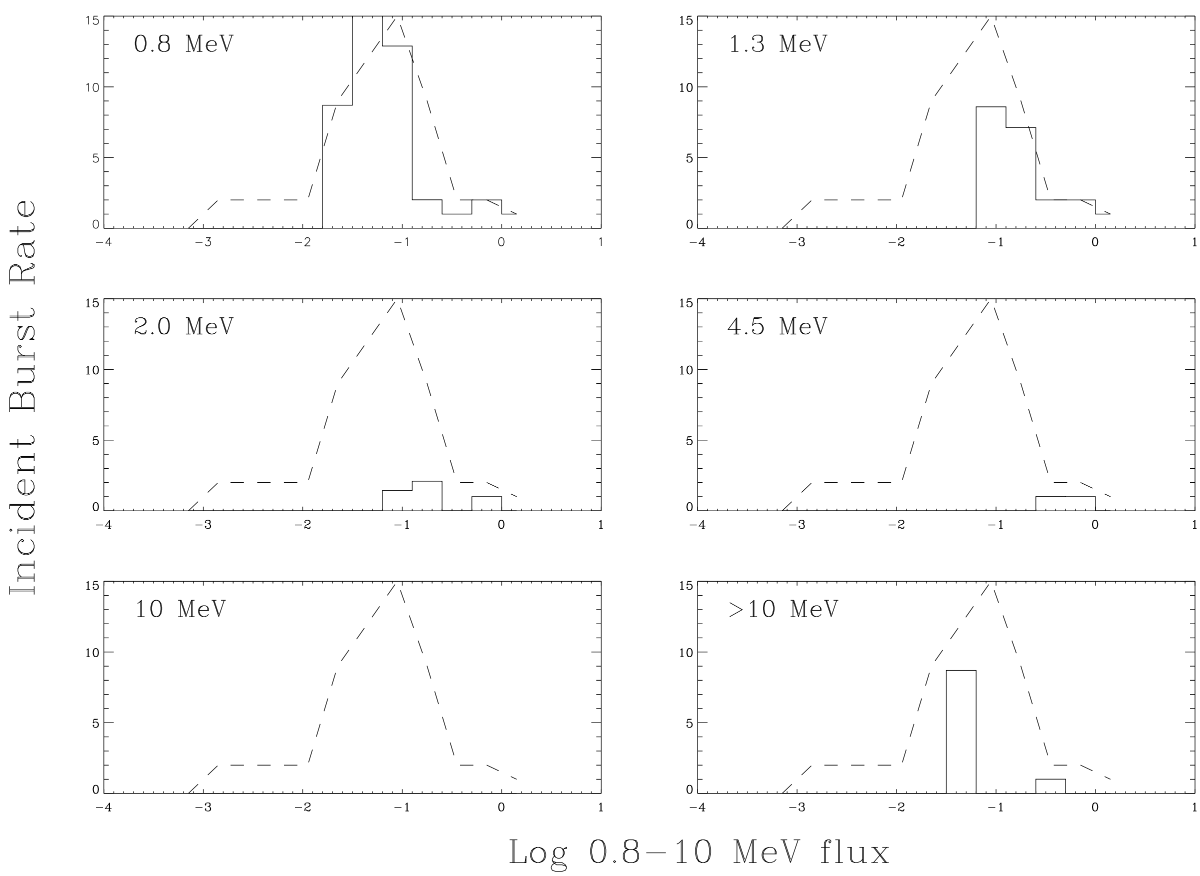

FIG. 6.—Sections through Fig. 4*a* at six constant values of spectral hardness. *Histogram:* Number of GRBs per bin of spectral hardness and flux detected by *SMM* (from Figs. 4*a* and 4*b*), corrected by the detection efficiencies in Fig. 5. *Dashed line: SMM* GRB rate expected from Piran & Narayan (1996), from Fig. 4*a*. Only GRBs with flux $\geq 5 \times 10^{-2}$ photons cm^{-2} s^{-1} are included in Table 1, which gives upper limits on the GRB rate for each H_0 value. Upper limits on the GRB rate for individual flux bins in the figure can be obtained by applying the same formulae (Gehrels 1986) to the rates in the bin.

TABLE 1

EXPECTED AND OBSERVED NUMBERS OF GRBS AS A FUNCTION OF SPECTRAL HARDNESS

Hardness Range (MeV)	Number of GRBs Detected	Number of GRBs Detected, Corrected for Sensitivity	Upper Limit on Corrected Detected Number[a]	Predicted Number
0.7–1.4	20	23.0	32.1	33.0
1.4–2.8	13	14.9	22.6	33.0
2.8–5.6	2	2.0	6.3	33.0
> 5.6	1	3.9	7.6	33.0

NOTE.—GRB range: 0.8–10 MeV flux ≥ 0.05 photons cm^{-2} s^{-1}.

[a] Poisson upper 95% confidence limit from Gehrels 1986.

for the GRS is far smaller than the number expected from the Piran & Narayan (1996) model. We have integrated under the histograms in Figure 6 for all GRBs brighter than an assumed threshold 5×10^{-2} photons cm^{-2} s^{-1} in order to present concisely the difference between the observations and the model. The results are given in Table 1. Our basic conclusion is that, relative to GRBs with hardness $H_0 \simeq 0.5$ MeV, those with $H_0 \simeq 2$ MeV are underabundant by at least 50%, and those with H_0 at any energy greater than 3 MeV are underabundant by at least a factor 5.

There therefore appears to be no large population of GRBs with hard spectra that have escaped detection due to a bias toward detection of softer spectra. This conclusion can only be avoided if such a population has properties considerably different from the known GRB population. For instance, it is possible that there is a population with hardnesses in the 0.8–10 MeV range, but which is abnormally faint (fluxes $\ll 0.05$ photons cm^{-2} s^{-1}). The BATSE detector is much more sensitive to faint bursts than the *SMM* GRS. However the analysis of BATSE spectra by Piran & Narayan (1996) suggests that, if anything, the opposite is true (i.e., the harder GRBs seen by BATSE are more luminous). Also, as noted in § 2.4, the subgroup of GRBs whose durations are ≤ 2 s is not well monitored by *SMM*, and a GRB population drawn exclusively from this subgroup can contain more hard bursts undetectable by the GRS (Kouveliotou et al. 1993). Finally, GRBs with durations greater than 100 s would also be difficult for the GRS to detect, and might contain an excess of hard bursts.

4. DISCUSSION

We have demonstrated that there is no large undiscovered class of GRBs with spectral hardness H (or peak in νf_ν) greater than 0.8 MeV. There is thus no need to invoke novel theoretical GRB mechanisms such as accretion-induced collapse of white dwarfs (Katz & Canal 1996) that might predict such a class. The two new hard events found in our search have spectral parameters similar to the harder members of the traditional GRB population (e.g., power-law indices ~ -1.0, compared to the hardest previous index ~ -1.3; Share et al. 1992), so that they are likely to be merely outlying members of that population.

Our results also cast doubt upon more conventional GRB models in which spectral peaks or breaks in νf_ν are expected to occur above 1 MeV. Such GRBs would have hardness $H > 1$ MeV, and our results constrain the frequency of these events. For example, less than one-seventh of the GRBs with νf_ν peaks above 0.7 MeV can have peaks at $\gtrsim 3$ MeV (Table 1). One class of models that is constrained is the cosmological fireball plus blast-wave model, which generally predicts multiple spectral breaks at energies up to TeV γ-rays, due to separate synchrotron and inverse Compton radiation mechanisms in forward and reverse shocks and in the blast wave (Mészáros, Rees, & Papathanassiou 1994). However, we are not aware that any calculation has been made of the relative frequency distribution of these breaks with energy up to 10 MeV, which might be quantitatively compared to our results. By contrast, there are other cosmological models in which peak or break energies are required by some physical mechanism to lie below ~ 1 MeV, in agreement with our result. In models involving within-source absorption (Brainerd 1994; Liang 1994) the physical mechanism is the energy dependence of the absorption cross section (respectively, Compton scattering and photoelectric absorption); in fireball plus shock-acceleration models (e.g., Tavani 1995), it is the electron rest energy of 0.511 MeV introducing relativistic effects into a synchrotron spectrum from accelerated e^--e^+ pairs.

5. SUMMARY

Our search of the 1981–1989 *SMM* GRS data at energies 0.8–10 MeV yielded only two possible GRBs having such hard spectra that they were discovered only at these energies but not in the lower 0.35–0.8 MeV band, which had been searched previously. We carefully examined the factors affecting the GRS's sensitivity, and concluded that this lack of detections is due to a real deficiency of GRBs with peaks in νf_ν or breaks above 0.7 MeV. The rate of GRBs in the overall *SMM* sample is highest for νf_ν peaks around $\simeq 0.5$ MeV. The rate of GRBs with peaks at any energy greater than 3 MeV is at least a factor of 5 lower than this maximum rate. These results favor GRB models in which some physical mechanism constrains burst hardnesses to be generally less than 1 MeV.

This work was supported by NASA Astrophysics Data Program grant NAG5-2721 and contract SG7048-F. We are grateful to Dan C. Messina for help with the data analysis.

REFERENCES

Band, D., et al. 1993, ApJ, 413, 281
Brainerd, J. J. 1994, ApJ, 428, 21
Dezalay, J. P., Lestrade, J. P., Barat, C., Talon, R., Sunyaev, R., Terekhov, O., & Kuznetsov, A. 1996, ApJ, 471, L27
Dingus, B. L. 1995, Ap&SS, 231, 187
Dunphy, P. P., Forrest, D. J., Chupp, E. L., & Share, G. H. 1989, in High-Energy Radiation Background in Space, ed. A. C. Rester, Jr. & J. I. Trombka (New York: AIP), 259
Fennimore, E. E., Klebesadel, R. W., Laros, J., Lacey, C., Madras, C., Meier, M., & Schwarz, G. 1993, *Compton Gamma Ray Observatory*, ed. M. W. Friedlander, N. Gehrels, & D. J. Macomb (New York: AIP), 744
Fishman, G. J., & Meegan, C. A. 1995, ARA&A, 33, 415
Gehrels, N. 1986, ApJ, 303, 336
Higdon, J. C., Matz, S. M., Share, G. H., Messina, D. C., & Iadicicco, A. 1992, in Proc. Huntsville Gamma-Ray Burst Workshop, ed. W. S. Paciesas & G. J. Fishman (New York: AIP), 89
Hurley, K. 1992, in Proc. Huntsville Gamma-Ray Burst Workshop, ed. W. S. Paciesas & G. J. Fishman (New York: AIP), 3
Hurley, K., et al. 1994, Nature, 372, 652
Katz, J. I., & Canel, L. M. 1996, ApJ, 471, 915
Kouveliotou, C., Meegan, C. A., Fishman, G. J., Bhat, N. P., Briggs, M. S., Koshut, T. M., Paciesas, W. S., & Pendleton, G. N. 1993, ApJ, 413, L101
Kurfess, J. D., et al. 1989, in High-Energy Radiation Background in Space, ed. A. C. Rester, Jr. & J. I. Trombka (New York: AIP), 259
Liang, E. P. 1994, in Proc. Second Huntsville Gamma-Ray Burst Workshop, ed. G. J. Fishman, J. J. Brainerd, & K. Hurley (New York: AIP), 351
Matz, S. M., Forrest, D. J., Vestrand, W. T., Chupp, E. L., Share, G. H., & Rieger, E. 1985, ApJ, 288, L37
Matz, S. M., Higdon, J. C., Share, G. H., Messina, D., C., & Iadicicco, A. 1992, in Gamma-Ray Bursts, ed C. Ho, R. I. Epstein, & E. E. Fenimore (Cambridge: Cambridge Univ. Press), 175
Messina, D. C., & Share, G. H. 1992, in Proc. Huntsville Gamma-Ray Burst Workshop, ed. W. S. Paciesas & G. J. Fishman (New York: AIP), 206
Mészáros, P., Rees, M. J., & Papathanassiou, H. 1994, ApJ, 432, 181
Nolan, P. L., Share, G. H., Chupp, E. L., Forrest, D. J., & Matz, S. M. 1984, Nature, 311, 360
Piran, T., & Narayan, R. 1996, in Proc. Third Huntsville Gamma-Ray Burst Workshop, ed. C. Kouveliotou, M. S. Briggs, & G. J. Fishman (New York: AIP), 233
Rieger, E., Vestrand, W. T., Forrest, D. J., Chupp, E. L., Kanbach, G., & Reppin, C. 1989, Science, 244, 441
Share, G. H., et al. 1982, in Gamma-Ray Transients and Related Astrophysical Phenomena, ed. R. E. Lingenfelter, H. S. Hudson, & D. M. Worrall (New York: AIP), 45
Share, G. H., Matz, S. M., Messina, D. C., Nolan, P. L., Chupp, E. L., Forrest, D. J., & Cooper, J. C. 1986, Adv. Space Res., 6(4), 15
Share, G. H., Kurfess, J. D., Marlow, K. W., & Messina, D. C. 1989, Science, 244, 444
Share, G. H., Messina, D. C., Iadicicco, A., Matz, S. M., Rieger, E., & Forrest, D. J. 1992, in Gamma-Ray Bursts, ed C. Ho, R. I. Epstein, & E. E. Fenimore (Cambridge: Cambridge Univ. Press), 249
Tavani, M. 1995, Ap&SS, 231, 181